

Neutrino mass limits: robust information from the power spectrum of galaxy surveys

Antonio J. Cuesta^{a*}, Viviana Niro^{b†}, Licia Verde^{acde‡}

^a*Institut de Ciències del Cosmos (ICCUB), Universitat de Barcelona (IEEC-UB),
Martí i Franquès 1, E08028 Barcelona, Spain*

^b*Departamento de Física Teórica, Universidad Autónoma de Madrid, and Instituto
de Física Teórica UAM/CSIC, Calle Nicolás Cabrera 13-15, Cantoblanco, E-28049 Madrid, Spain*

^c*ICREA (Institució catalana de recerca i estudis avançats)*

^d*Radcliffe Institute for Advanced Study & ITC,
Harvard-Smithsonian Center for Astrophysics, Harvard University, MA 02138, USA*

^e*Institute of Theoretical Astrophysics, University of Oslo, 0315 Oslo, Norway*

July 8, 2022

Abstract

We present cosmological upper limits on the sum of active neutrino masses using large-scale power spectrum data from the WiggleZ Dark Energy Survey and from the Sloan Digital Sky Survey -Data Release 7 (SDSS-DR7) sample of Luminous Red Galaxies (LRG). Combining measurements on the Cosmic Microwave Background temperature and polarisation anisotropies by the Planck satellite together with WiggleZ power spectrum results in a neutrino mass bound of 0.43 eV at 95% C.L., while replacing WiggleZ by the SDSS-DR7 LRG power spectrum, the 95% C.L. bound on the sum of neutrino masses improves to 0.17 eV. Adding Baryon Acoustic Oscillation (BAO) distance scale measurements, the neutrino mass upper limits greatly improve, since BAO data break degeneracies in parameter space. Within a Λ CDM model, we find an upper limit of 0.11eV (0.15 eV) at 95% C.L., when using SDSS-DR7 LRG (WiggleZ) together with BAO and Planck. The addition of BAO data makes the neutrino mass upper limit robust, showing only a weak dependence on the power spectrum used. We also quantify the dependence of neutrino mass limit reported here on the CMB lensing information. The tighter upper limit (0.11 eV) obtained with SDSS-DR7 LRG is very close to that recently obtained using Lyman-alpha clustering data, yet uses a completely different probe and redshift range, further supporting the robustness of the constraint. This constraint puts under some pressure the inverted mass hierarchy and favours the normal hierarchy.

*email: ajcuesta@icc.ub.edu

†email: viviana.niro@uam.es

‡email: liciaverde@icc.ub.edu

1 Introduction

Neutrino oscillation experiments, including solar, atmospheric, and reactor experiments, require that neutrinos have mass (Nobel Prize in Physics 2015; see for example Ref. [1, 2]). However, the neutrino mass hierarchy, normal or inverted, as well as the sum of the three active neutrino masses, are quantities that are still unknown.

Cosmology provides important information on the sum of neutrino masses, M_ν , since this quantity affects the expansion rate of the Universe and the way large-scale structures form and evolve.

Thus, an interplay between laboratory experiments and cosmology on neutrino masses can provide significant information on neutrino physics, e.g., Ref. [3, 4, 5] and refs. therein. It is from this interplay for example that cosmology helps determining also the mass hierarchy. Should the cosmological constraints of the sum of the masses bound $M_\nu < 0.1$ eV at reliable significance level, this would indicate a normal mass hierarchy and exclude the inverted one. This is why reaching the 0.1 eV precision (and accuracy) in M_ν is a highly desirable target and would have profound implications beyond cosmology. Considering the analysis of Ref. [1], the current minimum value allowed for an inverted hierarchy is $M_\nu = 0.0982 \pm 0.0010$ eV (68% C.L.).

Neutrino masses affect on the Cosmic Microwave Background (CMB) anisotropies through the Early Integrated Sachs Wolfe Effect, and they influence gravitational lensing measurements. Massive neutrinos, moreover, lead to a suppression on the matter power spectrum at small scales. For this reason, measurements of the full shape of the matter power spectrum are of great importance for neutrino physics since they are able to put tight constraints on the sum of neutrino masses.

This has been shown previously in the literature starting with the pioneering work of [6], see [7] for a review. Recently, using the WiggleZ (WZ) Dark Energy Survey galaxy power spectrum [8], it has been shown that WZ combined with Planck 2013 data can provide tight constraints on the sum of neutrino masses. Before WZ, the state-of-the art galaxy survey for neutrino mass analysis was the SDSS DR7, used e.g. in [9] or its photometric counterpart in [10]. To date the strongest constraint on M_ν is provided by the joint analysis of CMB, BAO and Lyman- α forest data [11, 12], $M_\nu < 0.12$ eV (95% C.L.), reaching tantalisingly close to the 0.1 eV target. The next generation of cosmological surveys have the statistical power to detect the signature of non-zero M_ν even if it had the minimum value allowed by oscillation measurements and the mass hierarchy was normal e.g., [13, 14, 15].

All these analyses use the power spectrum of dark matter tracers and thus rely on the assumption that it can be used as a proxy for the dark matter power spectrum itself. Galaxies are not expected to Poisson-sample the matter distribution; the galaxy-dark matter connection is complicated and not yet well understood; galaxies (or the intergalactic medium) are known to be biased tracers of the dark matter density field, and different tracers are known (see pioneering work by [16]) to cluster differently. Galaxy bias probably represent the main limitation in extracting constraints on neutrino masses from galaxy surveys, which can introduce potentially crippling systematic errors on this parameter as the upper limits shrink towards the 0.1 eV target. In Ref. [17] the authors address this issue by considering neutrino mass limits from the clustering of red and blue galaxies of the SDSS DR7 main sample. They find different upper limits between the two samples (by 0.22 eV) when both are combined with WMAP 5 years CMB power spectrum

data, which they interpret as broad agreement for their data set but a hint of a possible issue with galaxy bias for future data.

Here we perform a more extreme test by considering luminous red galaxies (LRG in DR7) and emission line galaxies (WZ). LRG are mostly passively evolving, massive galaxies thought to inhabit preferentially the centre of cluster-size dark matter halos [18, 19]. The WZ galaxies are star-forming blue galaxies which tend to avoid the densest regions (hence avoid the centre of cluster-size dark matter halos) [20]. Moreover the power spectrum extracted from the LRG catalog is an estimate of the power spectrum of the massive halos hosting the LRG galaxy population. Thus not only the bias of the two tracers are very different but also the sensitivity of their power spectra to non-linearities and non-linear redshift space distortions. Because of the extremely different properties of the tracers, agreement in the constraints obtained would signify that any systematic effects due to galaxy bias (and non-linearities) are below the reported error-bars.

In this paper not only for the first time we compare the constraints on neutrino masses obtained from the shape of the power spectrum of SDSS DR7 LRG galaxies and that of WZ galaxies, but also consider state-of-the art data from CMB observations of the Planck satellite (Planck 2015) [21] and BAO data. Note that precision of the Planck 2015 data has also greatly improved the sensitivity to test perturbations in the cosmic neutrino background, see for example the analysis in Refs. [22, 23, 21] (for the case of self-interacting neutrinos see instead the discussion in Refs. [24, 25]).

This paper is organised as follows: In Sect. 2 we present our methodology, in particular we describe the parameterisation adopted and the data sets considered. In Sect. 3 we present our results on the upper limit on the sum of neutrino masses from different data set combinations. We discuss our findings and compare them with other constraints presented in the literature. Finally we conclude in Sect. 4.

2 Methods and data

2.1 Model parameterization and fitting procedure

In our analysis, we consider the six parameters describing the Λ CDM model with the addition of the sum of active neutrino masses. We perform standard Bayesian inference using the following parameters:

$$\{\omega_b, \omega_{\text{cdm}}, 100\Theta_s, \ln(10^{10} A_s), n_s, \tau_{\text{reio}}, \sum m_\nu\}.$$

The first six cosmological parameters denote the physical baryon density ($\omega_b \equiv \Omega_b h^2$), the physical cold dark matter density ($\omega_{\text{cdm}} \equiv \Omega_{\text{cdm}} h^2$), the ratio between the sound horizon and the angular diameter distance at decoupling (Θ_s), the amplitude (A_s) of the power spectrum of primordial fluctuations at the pivot scale $k_* = 0.05/\text{Mpc}$, the power spectrum index (n_s) of the primordial density fluctuations, the optical depth to reionisation (τ_{reio}), and the sum of the three active neutrino masses ($\sum m_\nu \equiv M_\nu$).

We assume an uniform prior for all these parameters. In addition, we enforce a lower bound prior on τ_{reio} of 0.04 eV, since lower values of τ_{reio} would be inconsistent with observations on the Gunn-Peterson effect, see e.g., Ref. [26] but this prior does not affect our conclusions or our bounds. All nuisance parameters used in the likelihood codes are marginalized over. In principle since the

neutrino mass upper limit can constrain the specific neutrino hierarchy (i.e., normal or inverted) there could be a weak dependence of the results on the adopted hierarchy, see Ref. [8] and also the discussion in Ref. [12], in which specific analyses considering different neutrino ordering have been carried out. In our analysis, we consider three degenerate massive neutrinos, setting a lower bound equal to zero on M_ν . This choice is analogous to the one considered in the analysis of the Planck collaboration [21]. For the expected error-bars, this approximation introduces negligible errors. In this way, we can derive an independent upper limit set by cosmology on the total mass of active neutrinos, without considering the information reported by neutrino oscillation experiments. However, for future surveys with reduced error-bars the adopted hierarchy matters, see e.g., [13, 27] and refs therein.

We use the Cosmic Linear Anisotropy Solver Software (CLASS) ¹ presented in Ref. [28] for the solution of Boltzmann equations and the calculation of Cosmic Microwave Background and large scale structure observables. For the parameter inference we use the public code MONTE PYTHON ² described in Ref. [29]. This is based on a Metropolis Hastings algorithm and it uses a Cholesky decomposition in order to handle a large number of nuisance parameters [30].

Note that we will not consider extended cosmological models and their effect on the upper bound for the three active neutrino masses. In these more general cases, for example, relaxing spatial flatness, varying N_{eff} or adding a massive sterile neutrino $m_{\nu, \text{sterile}}^{\text{eff}}$ –see e.g., Refs. [31, 32, 33, 34, 35, 36] for constraints on sterile neutrinos from cosmology–, the bounds on the sum of the three active neutrino masses are, in general, less constraining. To understand how these different assumptions might affect the neutrino mass bounds, we refer to Ref. [21], see also Ref. [4] for a previous study on this topic. Finally, constraints on neutrino masses could change also in the presence of cosmological axions. For a recent analysis on this topic, using the Planck 2015 data release, see Ref. [37], see also Ref. [38] for the impacts of dark energy on neutrino upper limits.

2.2 Data sets

In the following we outline the data sets used.

Cosmic Microwave Background:

We use information on the CMB from the Planck 2015 data releases. When analyzing the recent Planck 2015 measurements of temperature and polarization anisotropies [21], we consider a combination of the likelihood at $l \geq 30$ using TT, TE and EE power spectra and the Planck low-multipole temperature+polarization likelihood at $l \leq 29$. This combination has been referred as Planck TT,TE,EE+lowP in Ref. [21]. In the following, we will use the nomenclature of “CMB15” to refer to these combination of data. We also include the Planck 2015 lensing likelihood, as constructed from measurements of the power spectrum of the lensing potential $C_l^{\phi\phi}$ [39].

Power spectrum $P(k)$:

We use the power spectrum of the halo density field derived by [40] from a sample of Luminous

¹<http://class-code.net>

²<http://montepython.net/>

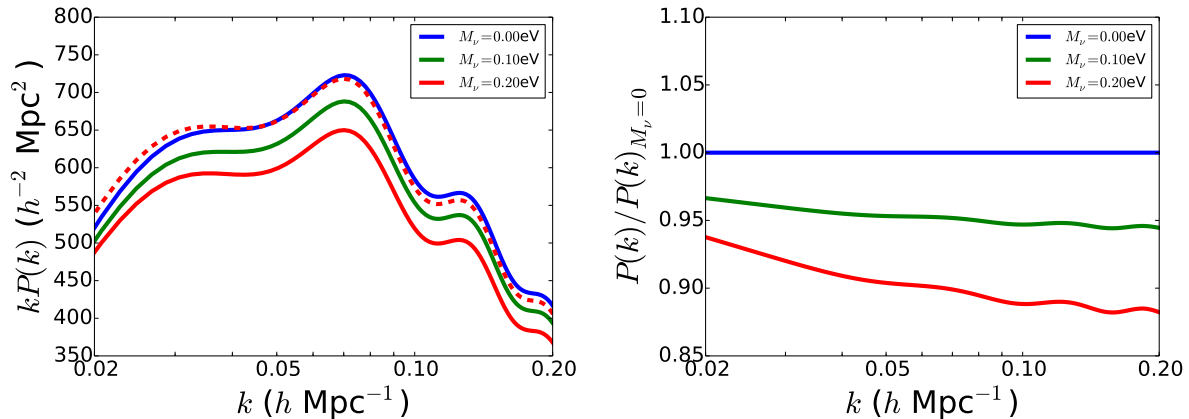


Figure 1: Effect (absolute on the left panel and relative to the massless neutrino case on the right panel) of neutrino mass on the non-linear matter power spectrum at $z = 0$ for the k -range used in this analysis, prior to applying the window function of the survey. Shown are the power spectrum for massless neutrinos (blue), for the neutrino mass close to the bound in this paper (green), and for the neutrino mass close to the bound given by current CMB+BAO data (red) while Ω_m and all other cosmological parameters (except for ω_{cdm}) are kept fixed. The dashed red line is the red line renormalized (akin to a scale-independent bias factor) to match the blue one at $k = 0.05 h \text{ Mpc}^{-1}$.

Red Galaxies in the Sloan Digital Sky Survey DR7 (LRG). The scales probed by this measurement range from $k = 0.02 h \text{ Mpc}^{-1}$ to $0.2 h \text{ Mpc}^{-1}$.

We have rewritten the original likelihood code ³ into Python so that we could interface it through MONTEPYTHON. The treatment of non-linearities is analogous to the original code, in which the linear matter power spectrum is fed into HALOFIT to compute non-linear effects, and a smooth polynomial derived from N -body simulations is used to account for additional scale-dependent effects between the halo power spectrum and matter power spectrum. However, since in our case we are using an updated, more accurate version of Halofit [41, 42] which models the effects on massive neutrinos in the non-linear corrections⁴, we recomputed the non-linear $P(k)$ ratios for their fiducial cosmology and replaced the original files with these updated templates. In order to do so, we have used the code COSMOLOPY ⁵ interfaced by the code HMF ⁶[43]. As in the original code, we also include the (redshift-dependent) effect of BAO smoothing due to non-linear evolution.

We use also power spectrum data from the WiggleZ Dark Energy Survey [44], that consists of galaxies in a redshift range $z < 1.0$. For detailed information on the WZ survey and data releases, see also Refs. [45, 46] We restrict the analysis to $k < k_{\text{max}} = 0.2 h \text{ Mpc}^{-1}$, to minimize the uncertainties in the modelling of the non-linear regime as shown in Ref. [47, 8].

³<http://lambda.gsfc.nasa.gov/toolbox/lrgdr/>

⁴In the original likelihood, the halofit version adopted did not account for massive neutrinos.

⁵<http://roban.github.com/CosmoLoPy/>

⁶<https://github.com/steven-murray/hmf>

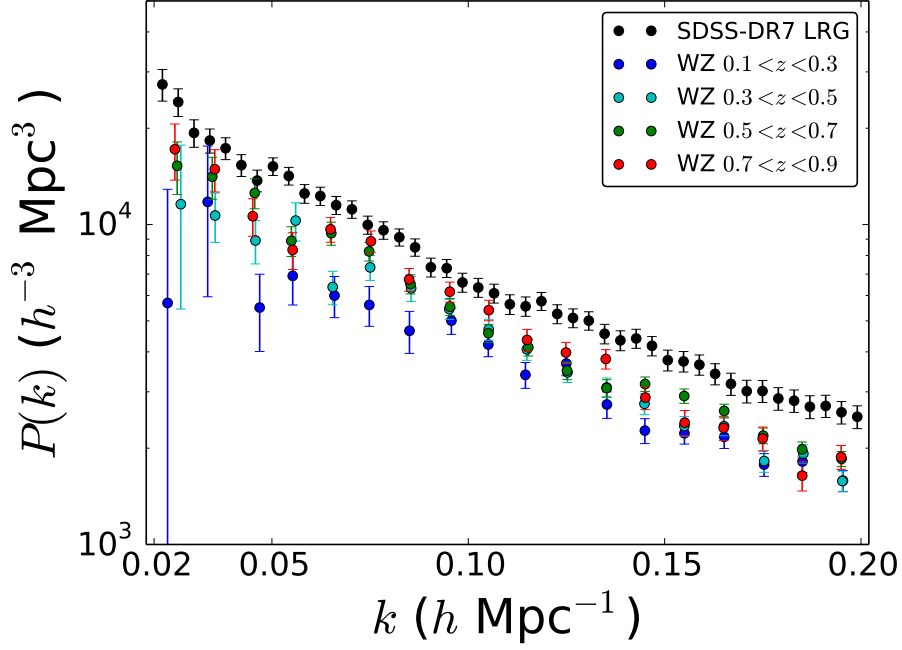


Figure 2: LRG and WZ data sets used. The LRG data are at $z \sim 0.35$ and WZ is separated in four redshift bins at effective redshifts $z = 0.22, 0.41, 0.6, 0.78$, only band powers with $k < 0.2 \ h \text{ Mpc}^{-1}$ are used here. A visual comparison of the two data sets might be misleading since not only the galaxy samples but also the window functions of the two surveys are different.

The non-linear matter power spectrum at $z = 0$ over the range of scales used here is shown in Fig.1 for several values of M_ν . The power spectra for LRG and WZ data are shown in Fig. 2.

Baryon Acoustic Oscillations:

BAO measurements greatly help to lift cosmological parameters degeneracies (in particular by ruling out small values of H_0 allowed by the CMB-only case) which affect constraints obtained from CMB data. Specifically, we use the recent determinations of D_V/r_{drag} as reported by the analysis of the Six-degree-Field Galaxy Survey (6dFGS) [48], the SDSS Main Galaxy Sample (MGS) [49], the Baryon Oscillation Spectroscopic Survey (BOSS) LOWZ and CMASS samples [50], where we use the anisotropic BAO measurement in the case of CMASS. Note that the BAO data used in our analysis are different from the one used in Ref. [8] and from the ones used by Planck collaboration in the 2013 release [51]. These BAO data sets correspond to those used recently by Planck collaboration in the 2015 release [21]. When we combine BAO information with the full matter power spectrum data from the SDSS-DR7 LRG, we have not added the SDSS-MGS BAO data set of Ref. [49], to avoid possible double counting of information.

We did not use in this study the information from Lyman- α forest BAO data [52].

Data sets	M_ν at 95% CL
CMB15 + LRG (+lensing)	0.17 eV (0.19 eV)
CMB15 + LRG + BAO (+lensing)	0.11 eV (0.12 eV)
CMB15 + WZ (+lensing)	0.43 eV (0.49 eV)
CMB15 + WiggleZ + BAO (+lensing)	0.15 eV (0.18 eV)
CMB15 + LRG + WZ (+lensing)	0.16 eV (0.18 eV)
CMB15 + LRG + WZ + BAO (+lensing)	0.11 eV (0.12 eV)

Table 1: Upper bounds (at 95% C.L.) on the sum of the three active neutrino masses, M_ν , for different combinations of data sets. With CMB15 we indicate the combination of Planck TT,TE,EE + lowP data, while LRG and WZ designate the full shape of the matter power spectra as reported by SDSS-DR7 and WiggleZ survey respectively. For the detailed description of the single data set used, we refer to Sec. 2.2.

3 Results

In Table 1, we report the limits at 95% C.L. on the sum of neutrino masses (assuming, as standard, three active neutrinos) as obtained using recent data from the Planck experiment and Large Scale Structure measurements from WZ and LRG (see Fig.3). In our runs we focus on the CMB15 combination of data, since we want to see explicitly how polarization data changes the bound on the neutrino masses. In Ref. [21], an upper bound of $M_\nu < 0.49$ eV (0.59 eV) was reported for the combination CMB15(+lensing). We find that adding the information from the LRG sample improves the limits to 0.17 eV (0.19 eV), while when considering the WZ data set, we find an upper limit of 0.43 eV (0.49 eV). We can see that when adding information from lensing, the neutrino upper bounds are slightly worse, and that the LRG data set is giving tighter constraints respect to the WZ data set. This will be further explored below.

For the combination of CMB15+BAO, the upper limit reported by the Planck collaboration on the sum of neutrino masses improves to $M_\nu < 0.17$ eV at 95% C.L. [21]. We find that, when adding BAO data to the LRG information, the bound decreases to 0.11 eV, and to 0.12 eV if the CMB lensing information is also included. Considering, instead, the WZ information combined with BAO, we find compatible upper limits of 0.15 eV, and 0.18 eV when the lensing information is also included. The constraints on the values of the remaining cosmological parameters allowed to vary in our analysis are summarized in Table 2.

In Fig.4, we illustrate the M_ν posterior distribution considering CMB15 combined with either LRG (left panel) or WZ (right panel). It can be clearly seen how BAO information tightens the neutrino masses upper limits, providing a great improvement especially to the WZ data set. In order to clarify how future cosmological measurements can help break further the degeneracies in neutrino mass measurements, we report the likelihood contours for all the relevant cosmological parameters (M_ν , τ_{reio} , H_0 , and σ_8) for the combination of CMB15+LRG+BAO and Planck+WZ+BAO in Fig. 5. The effect of combining both galaxy surveys is shown in Fig. 6 and in Fig. 7, and the M_ν bounds are reported in Table 1. We note that adding WZ to LRG does not change the constraints.

We can conclude that, if the BAO information is not included, LRG provides a significantly

Parameter	CMB15+LRG+BAO	CMB15+WZ+BAO
$100 \omega_b$	$2.237^{+0.015}_{-0.014}$	$2.236^{+0.014}_{-0.015}$
ω_{cdm}	0.1182 ± 0.0011	0.1184 ± 0.0011
n_s	0.9684 ± 0.0042	$0.9671^{+0.0040}_{-0.0044}$
τ_{reio}	$0.083^{+0.014}_{-0.016}$	$0.079^{+0.016}_{-0.017}$
$\ln(10^{10} A_s)$	$3.098^{+0.028}_{-0.032}$	$3.089^{+0.032}_{-0.034}$
H_0	$68.20^{+0.54}_{-0.53}$	$67.98^{+0.55}_{-0.54}$
σ_8	0.834 ± 0.013	$0.827^{+0.016}_{-0.015}$
M_ν [eV]	< 0.11	< 0.15

Table 2: Constraints on the values of the cosmological parameters from CMB15+LRG+BAO and CMB15+WZ+BAO. With CMB15 we indicate the combination of Planck TT,TE,EE + lowP data, while LRG and WZ designate the full shape of the matter power spectra as reported by SDSS-DR7 and WiggleZ survey respectively. For the detailed description of the data set used, we refer to Sec. 2.2. For the total neutrino mass M_ν we report the 95% C.L. upper limit, whereas for all the other parameters we quote the mean values and 1σ error bars.

stronger upper limit on the sum of neutrino masses than WZ. When including BAO data, constraints are tighter and less dependent on the galaxy survey considered. However, even in this case the upper limit found for the combinations of CMB15+LRG+BAO is stronger than the one found considering CMB15+WZ+BAO. Our results for the CMB15+LRG+BAO data set combination are competitive with the strongest upper limit on neutrino masses presented in the literature, that is the value of $M_\nu < 0.12$ eV at 95% C.L. [12], obtained using Lyman- α data from the BOSS survey together with the recent Planck 2015 release and BAO data. This is an important result that shows how cosmology is pointing towards a similar value for the upper limit on the sum of neutrino masses M_ν , independently of the large-scale structure probe considered. Poorly known astrophysical processes are the main limitation in extracting constraints on neutrino masses from large-scale structures. Different tracers of the large scale structure are affected by different astrophysical processes: the fact that approaches as different as the one of [12] and the one presented here find consistent results, supports the robustness of the reported limit.

We find a very weak (if any at all) correlation between the parameter τ_{reio} and M_ν . On the other hand Fisher-based forecasts for future data, see e.g., [53, 54] find a correlation between the two parameters albeit of different degree and orientation depending on the specific experimental set up. It seems that stronger constraints on the expansion history than those adopted here are responsible for creating a correlation between these two parameters. In fact we can approximately reproduce the correlation found by [54] if we consider an extended data set including CMB15+BAO, the latest supernovae data compilation JLA [55] and the H_0 determination [56, 57]. The degeneracy arises because of the A_s vs $\exp(-2\tau)$ CMB degeneracy, which is partly broken by polarization information; the remaining degeneracy however propagates through M_ν . Here we have decided not to combine together too many datasets, and thus we do not find any significant correlation. It remains to be explored whether for future data, adding information on the power spectrum shape coming from large-scale structure data would break the $\tau_{reio} - M_\nu$ degeneracy.

It is mandatory to discuss why the LRG constraints on M_ν are stronger than the WZ constraints. WZ covers a larger volume (the effective volume of WZ is $V_{\text{eff}} = 0.34h^{-3}\text{Gpc}^3$ and LRG cover $V_{\text{eff}} = 0.26h^{-3}\text{Gpc}^3$). Since the errors on the power spectrum measurements scale like $V_{\text{eff}}^{-1/2}$ for this argument WZ is expected to produce slightly tighter constraints. However, since one must marginalize over an (unknown) galaxy bias amplitude, the sensitivity of large-scale structure data to M_ν is due to a measurement of the broadband shape of the power spectrum over the scales probed by the galaxy surveys. Here is where a narrow survey window function helps. The survey window function couples Fourier modes, transferring power from k to k' thus smoothing out features. For M_ν of 0.1 eV the power suppression (compared to the massless case) is $\sim 3.5\%$ at $k = 0.02h/\text{Mpc}$ and $\sim 5\%$ at $k = 0.2h/\text{Mpc}$ i.e., a $\sim 2\%$ effect. For reference, over the same k -range, the matter $P(k)$ drops by more than an order of magnitude, so even a transfer of $\sim 0.1\%$ of power between these two scales completely swamps the signal. In Fig. 8 we show the window functions of LRG and WG where it is possible to appreciate that the WZ window functions have broader wings than the LRG ones. This can be understood by considering the two surveys geometry: LRG covers 7931 square degrees of which 7190 are contiguous –and three redshift bins combined into a single redshift measurement of $P(k)$ – while WG covers 1000 square degrees divided in 7 disconnected patches and 4 redshift bins.

We have decided not to include in our analysis results from galaxy weak lensing surveys, like CFHTLenS [58, 59], since a tension is present with the base ΛCDM model (see discussion in [60, 39]). This discrepancy might be partially alleviated by extended models, with massive neutrinos and varying N_{eff} (for other analysis in this direction, using also data from Redshift Space Distortion and Baryon Acoustic Oscillation information, we refer to Ref. [61] and Ref. [62]). However, it was concluded in Ref. [60, 39] that modifications to the neutrino sector alone cannot resolve the tension and that further investigation into systematic effects or interpretation of the data is needed. For this reason, we decided to use the full shape information on the matter power as probed by galaxy redshift surveys instead.

4 Conclusions

It has long been recognized that cosmology can provide key information to learn about neutrino physics, most notably by constraining the neutrino absolute mass scale. However it is only very recently that the accuracy of cosmological measurements has reached a level where it could be used to determine the hierarchy and/or detect the effect of neutrino masses on the evolution of the universe and thus provide a measurement of the sum of the masses M_ν . In fact oscillation experiments impose a minimum M_ν for the inverted hierarchy around $M_\nu \gtrsim 0.1$ eV (e.g., [3]), and cosmological bounds are now reaching this level of accuracy. However accuracy is not enough: for cosmological constraints, to reach this level information about the clustering of large-scale structure, tracers such as the Lyman-alpha forest or galaxies must be included. These tracers are believed to be affected by poorly known astrophysics which makes them biased tracers with a poorly known bias. Thus these constraints should be shown to be also robust.

In this paper, we have analyzed the robustness of the neutrino mass upper limit under different combinations of data sets. In particular, we have focused our analysis on the constraints from

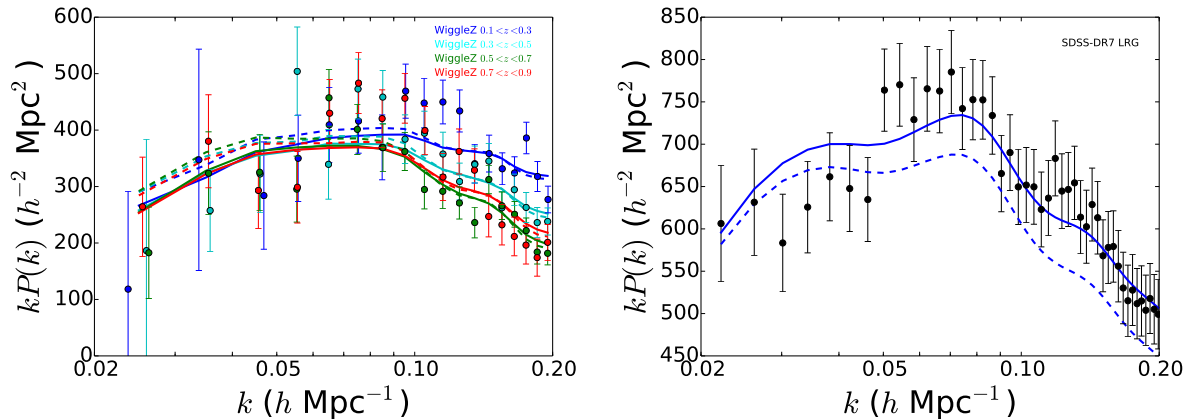


Figure 3: WZ (left) and LRG (right) data sets used and the theoretical best-fit obtained from CMB+ $P(k)$ data (solid line). The dashed line corresponds to a model with M_ν corresponding to the 95% limit for combination of CMB and the respective clustering data, keeping all other parameters fixed except for ω_{cdm} . The WZ plot is normalized so that all the lines overlap at large scales.

different galaxy power spectrum data. We have analysed in detail the information provided by two data sets, namely the WiggleZ Dark Energy Survey (WZ) and the Luminous Red Galaxies (LRG) sample of the SDSS-DR7. We have combined the information on the full shape of the matter power spectrum from these two data sets with the recent data from the Planck 2015 release and state-of-the-art BAO data.

The analysis presented here serves two purposes. Firstly we have demonstrated the level of robustness of the neutrino mass constraints obtained including galaxy clustering information. LRG galaxies are thought to inhabit preferentially the centre of cluster-size dark matter halos which populate high-density regions while WZ ones tend instead to avoid the densest regions. Thus not only the bias of the two tracers are very different but also the sensitivity of their power spectra to non-linearities. When including BAO data which reduce cosmological degeneracies present in CMB constraints, the LRG data set yields an upper limit of 0.11 at 95% C.L., while WZ an upper limit of 0.15 eV. While the WZ clustering measurements provide weaker constraints which we attribute to the nature of the survey window function, we conclude that systematic effects due to galaxy bias or non-linearities are safely below the error bars for the WZ limit.

Secondly we note that the LRG limit ($M_\nu < 0.11$ eV) is very close to the tightest limit in the literature, that corresponds to 0.12 eV obtained using the Lyman- α power spectrum from BOSS [12]. The Lyman- α signal corresponds to a yet completely different clustering tracer, mapping out the neutral Hydrogen in intergalactic medium. This further supports the robustness of the reported limit. This limit is reaching tantalizingly close to the 0.1 eV target corresponding to roughly the minimum M_ν allowed for active neutrinos with inverted hierarchy.

It was described in Ref. [63] how the constraints on M_ν can provide information on the neutrino mass degeneracy. The authors concluded that a bound of $M_\nu < 0.23$ eV was able to reject at 95% C.L. neutrino mass degeneracy larger than 85% (82.5%) for normal (inverted) hierarchy. The

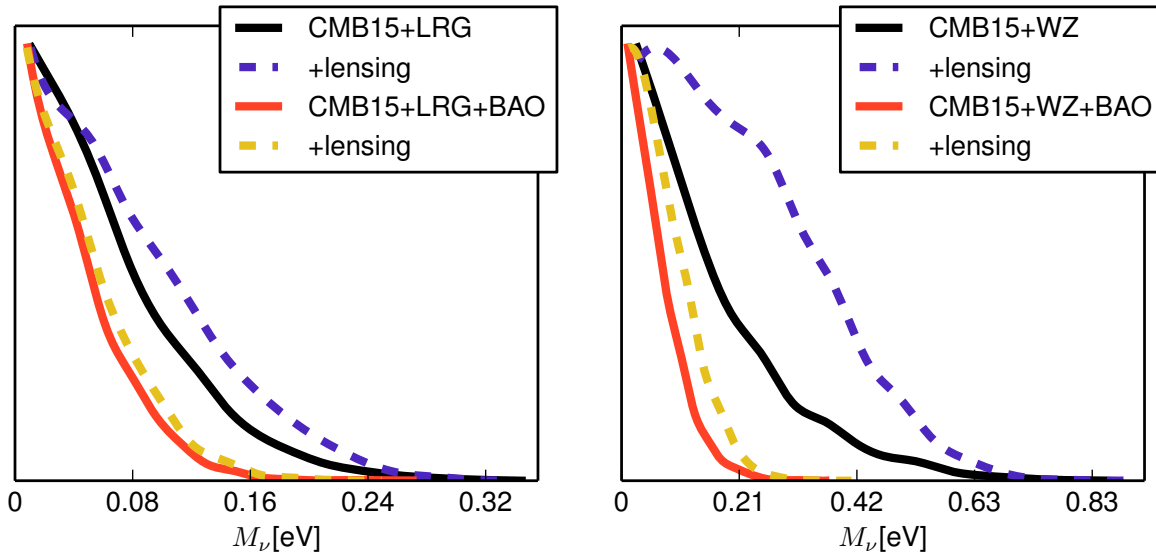


Figure 4: Comparison between the posterior distribution of the sum of neutrino masses, M_ν , from the following data combinations: CMB15 + LRG (+lensing) and CMB15 + LRG + BAO (+lensing), in the left panel; CMB15 + WiggleZ (+lensing) and CMB15 + WiggleZ + BAO (+lensing), in the right panel. CMB15 indicates the 2015 Planck TT,TE,EE + lowP data. For a detailed description of the individual data sets used, we refer to Sec. 2.2. We use black (blue dashed) lines when power spectrum data are combined with CMB15 (+lensing) data and red (yellow dashed) lines when also BAO is added.

bounds of 0.11 eV and 0.15 eV found in this work further support the conclusion of Ref. [63] and the constraints on the magnitude of degeneracy for neutrino masses. Moreover, Fig. 3 of Ref. [63] interpreted in light of the present constraint, indicates that neutrinoless double beta decay experiments should strive to reach ton-size detectors.

As a consequence, only a very small region of parameter space for the inverted hierarchy is still allowed, and even a modest improvement in current constraints could determine the hierarchy. Conversely, if the mass hierarchy is the inverted one, then a detection of neutrino mass from the sky and determination of the mass scale is just around the corner.

In conclusion, the information on the full shape of the matter power spectrum, accessible from large-scale structure with narrow window functions, is becoming of fundamental importance for neutrino physics and in particular in shedding light on the mass scale and the hierarchy.

Acknowledgements

We acknowledge Signe Riemer-Sørensen for discussions on the WiggleZ data analysis. LV and AJC are supported by the European Research Council under the European Community's Seventh Framework Programme FP7-IDEAS-Phys.LSS 240117. Funding for this work was partially

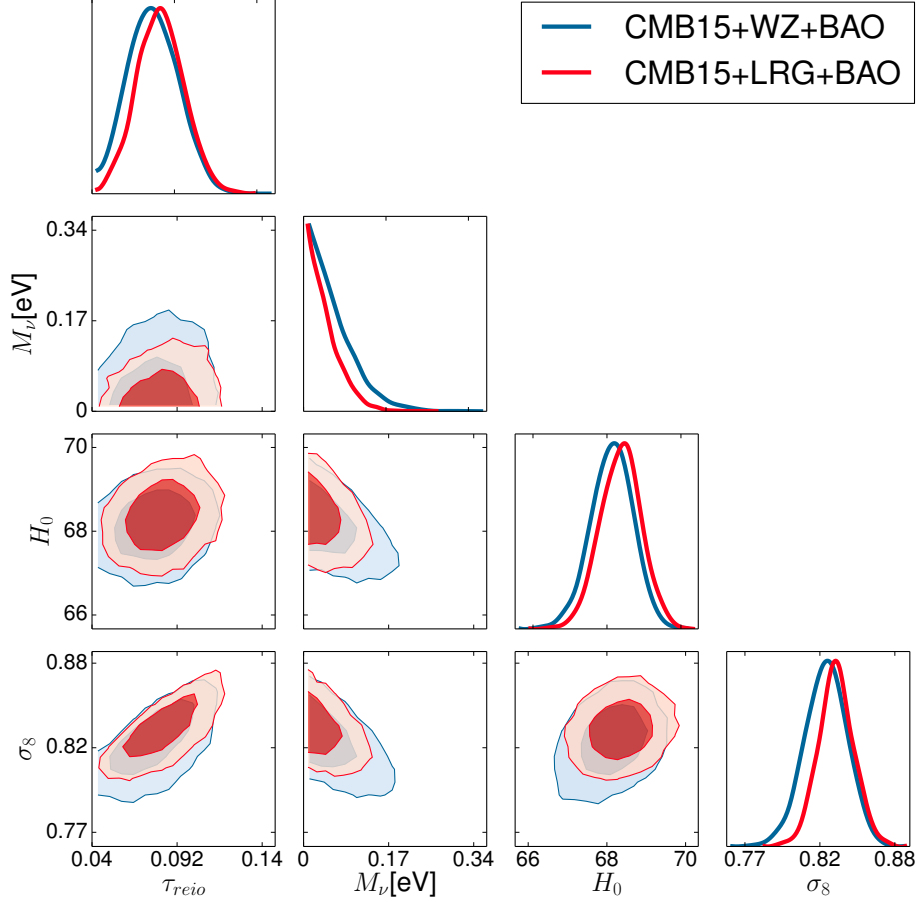


Figure 5: Two-dimensional posterior distribution for $(\tau_{reio}, M_\nu, H_0, \sigma_8)$ parameters from the CMB15 + LRG + BAO (red contours) and CMB15 + WZ + BAO (blue contours) datasets. The 1σ and 2σ contours are shown.

provided by the Spanish MINECO under projects FPA2011-29678-C02-02 and MDM-2014-0369 of ICCUB (Unidad de Excelencia 'María de Maeztu'). AJC acknowledges hospitality of ITC, Harvard-Smithsonian Center for Astrophysics, Harvard University. VN acknowledges support by Spanish MINECO through project FPA2012-31880, by Spanish MINECO (Centro de excelencia Severo Ochoa Program) under grant SEV-2012-0249 and by the European Union through the FP7 Marie Curie Actions ITN INVISIBLES (PITN-GA-2011-289442). The work of VN was also supported by the Deutsche Forschungsgemeinschaft (DFG) through the Collaborative Research Centre SFB 676 "Particles, Strings and the Early Universe" (through an SFB fellowship). VN would like to express a special thanks to the Mainz Institute for Theoretical Physics (MITP) for its hospitality and support.

Based on observations obtained with Planck (<http://www.esa.int/Planck>), an ESA science mission with instruments and contributions directly funded by ESA Member States, NASA, and Canada.

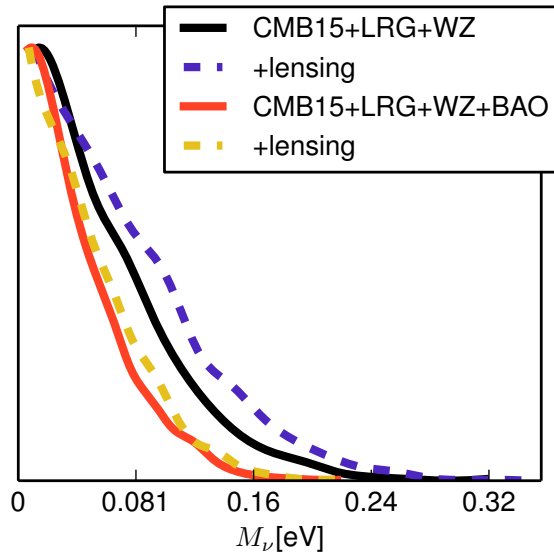


Figure 6: Comparison between the posterior distribution of the sum of neutrino masses, M_ν , from the following data combinations: CMB15 + LRG + WiggleZ (+lensing) and CMB15 + LRG + WiggleZ + BAO (+lensing). CMB15 indicates the 2015 Planck TT,TE,EE + lowP data. For a detailed description of the individual data sets used, we refer to Sec. 2.2. We use black (blue dashed) lines when power spectrum data are combined with CMB15 (+lensing) data and red (yellow dashed) lines when also BAO is added.

References

- [1] M. C. Gonzalez-Garcia, M. Maltoni, and T. Schwetz, JHEP **11**, 052 (2014), 1409.5439.
- [2] J. Bergstrom, M. C. Gonzalez-Garcia, M. Maltoni, and T. Schwetz (2015), 1507.04366.
- [3] R. Jimenez, T. Kitching, C. Peña-Garay, and L. Verde, JCAP **5**, 035 (2010), 1003.5918.
- [4] M. Gonzalez-Garcia, M. Maltoni, and J. Salvado, JHEP **1008**, 117 (2010), 1006.3795.
- [5] M. Gerbino, M. Lattanzi, and A. Melchiorri (2015), 1507.08614.
- [6] W. Hu, D. J. Eisenstein, and M. Tegmark, Phys. Rev. Lett. **80**, 5255 (1998), astro-ph/9712057.
- [7] J. Lesgourgues and S. Pastor, Phys. Rept. **429**, 307 (2006), astro-ph/0603494.
- [8] S. Riemer-Sørensen, D. Parkinson, and T. M. Davis, Phys.Rev. **D89**, 103505 (2014), 1306.4153.
- [9] B. A. Reid, L. Verde, R. Jimenez, and O. Mena, JCAP **1001**, 003 (2010), 0910.0008.

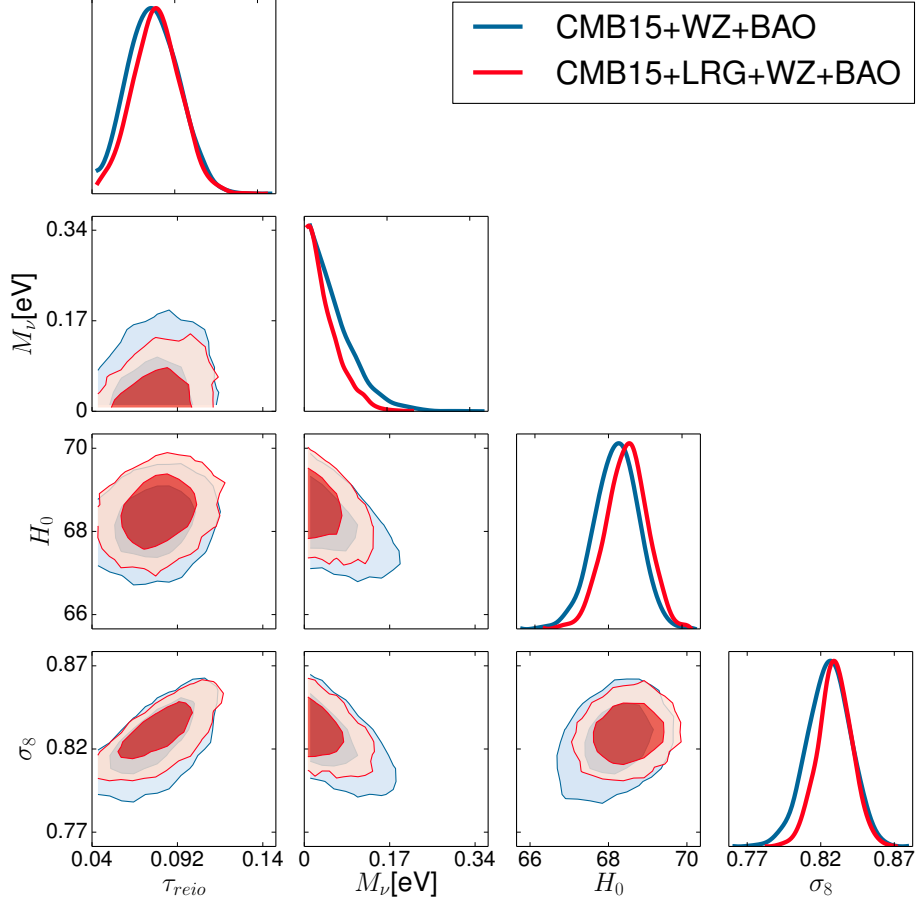


Figure 7: Two-dimensional posterior distribution for $(\tau_{reio}, M_\nu, H_0, \sigma_8)$ parameters from the CMB15 + LRG + WZ + BAO (red contours) and CMB15 + WZ + BAO datasets (blue contours). The 1σ and 2σ contours are shown.

- [10] S. A. Thomas, F. B. Abdalla, and O. Lahav, Phys. Rev. Lett. **105**, 031301 (2010), 0911.5291.
- [11] N. Palanque-Delabrouille *et al.*, JCAP **1502**(02), 045 (2015), 1410.7244.
- [12] N. Palanque-Delabrouille *et al.* (2015), 1506.05976.
- [13] C. Carbone, L. Verde, Y. Wang, and A. Cimatti, JCAP **1103**, 030 (2011), 1012.2868.
- [14] B. Audren, J. Lesgourgues, S. Bird, M. G. Haehnelt, and M. Viel, JCAP **1301**, 026 (2013), 1210.2194.
- [15] J. Hamann, S. Hannestad, and Y. Y. Y. Wong, JCAP **1211**, 052 (2012), 1209.1043.
- [16] M. Davis and M. J. Geller, ApJ **208**, 13 (1976).
- [17] M. E. C. Swanson, W. J. Percival, and O. Lahav, MNRAS **409**, 1100 (2010), 1006.2825.

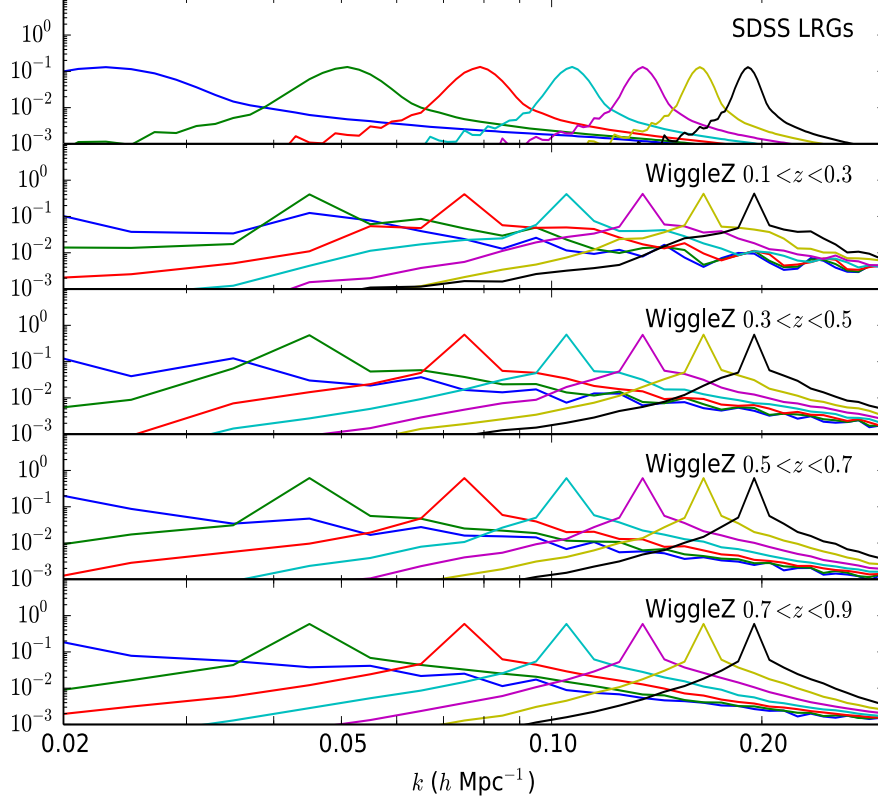


Figure 8: Window functions for a sample of k -bins, for LRG (top panel) and the four redshift bins of WZ (bottom four panels).

- [18] D. J. Eisenstein, J. Annis, J. E. Gunn, A. S. Szalay, A. J. Connolly, R. C. Nichol, N. A. Bahcall, M. Bernardi, S. Burles, F. J. Castander, M. Fukugita, D. W. Hogg, *et al.*, *AJ* **122**, 2267 (2001), [astro-ph/0108153](#).
- [19] B. A. Reid, D. N. Spergel, and P. Bode, *ApJ* **702**, 249 (2009), [0811.1025](#).
- [20] M. J. Drinkwater, R. J. Jurek, C. Blake, D. Woods, K. A. Pimbblet, K. Glazebrook, R. Sharp, M. B. Pracy, S. Brough, M. Colless, W. J. Couch, S. M. Croom, *et al.*, *MNRAS* **401**, 1429 (2010), [0911.4246](#).
- [21] P. A. R. Ade *et al.* (Planck) (2015), [1502.01589](#).
- [22] B. Audren *et al.*, *JCAP* **1503**, 036 (2015), [1412.5948](#).
- [23] E. Sellentin and R. Durrer, *Phys. Rev. D* **92**(6), 063012 (2015), [1412.6427](#).
- [24] F.-Y. Cyr-Racine and K. Sigurdson (2013), [1306.1536](#).

- [25] I. M. Oldengott, C. Rampf, and Y. Y. Y. Wong (2014), 1409.1577.
- [26] J. Caruana, A. J. Bunker, S. M. Wilkins, E. R. Stanway, S. Lorenzoni, M. J. Jarvis, and H. Ebert, Mon. Not. Roy. Astron. Soc. **443**(4), 2831 (2014), 1311.0057.
- [27] T. D. Kitching, A. F. Heavens, L. Verde, P. Serra, and A. Melchiorri, Physical Review D **77**(10), 103008 (2008), 0801.4565.
- [28] J. Lesgourgues (2011), 1104.2932.
- [29] B. Audren, J. Lesgourgues, K. Benabed, and S. Prunet, JCAP **1302**, 001 (2013), 1210.7183.
- [30] A. Lewis, Phys.Rev. **D87**, 103529 (2013), 1304.4473.
- [31] M. Archidiacono, N. Fornengo, C. Giunti, S. Hannestad, and A. Melchiorri, Phys. Rev. **D87**(12), 125034 (2013), 1302.6720.
- [32] J. Bergström, M. C. Gonzalez-Garcia, V. Niro, and J. Salvado, JHEP **10**, 104 (2014), 1407.3806.
- [33] S. Gariazzo, C. Giunti, and M. Laveder, JHEP **11**, 211 (2013), 1309.3192.
- [34] A. Mirizzi, G. Mangano, N. Saviano, E. Borriello, C. Giunti, G. Miele, and O. Pisanti, Phys. Lett. **B726**, 8 (2013), 1303.5368.
- [35] L. Verde, S. M. Feeney, D. J. Mortlock, and H. V. Peiris, JCAP **9**, 013 (2013), 1307.2904.
- [36] S. M. Feeney, H. V. Peiris, and L. Verde, JCAP **4**, 036 (2013), 1302.0014.
- [37] E. Di Valentino, E. Giusarma, M. Lattanzi, O. Mena, A. Melchiorri, and J. Silk (2015), 1507.08665.
- [38] X. Zhang (2015), 1511.02651.
- [39] P. A. R. Ade *et al.* (Planck) (2015), 1502.01591.
- [40] B. A. Reid *et al.*, Mon. Not. Roy. Astron. Soc. **404**, 60 (2010), 0907.1659.
- [41] R. Takahashi, M. Sato, T. Nishimichi, A. Taruya, and M. Oguri, Astrophys. J. **761**, 152 (2012), 1208.2701.
- [42] S. Bird, M. Viel, and M. G. Haehnelt, Mon. Not. Roy. Astron. Soc. **420**, 2551 (2012), 1109.4416.
- [43] S. Murray, C. Power, and A. Robotham (2013), 1306.6721.
- [44] D. Parkinson, S. Riemer-Sorensen, C. Blake, G. B. Poole, T. M. Davis, *et al.*, Phys.Rev. **D86**, 103518 (2012), 1210.2130.

- [45] C. Blake, S. Brough, M. Colless, W. Couch, S. Croom, *et al.*, Mon.Not.Roy.Astron.Soc. **406**, 803 (2010), 1003.5721.
- [46] M. J. Drinkwater, R. J. Jurek, C. Blake, D. Woods, K. A. Pimbblet, *et al.*, Mon.Not.Roy.Astron.Soc. **401**, 1429 (2010), 0911.4246.
- [47] S. Riemer-Sorensen *et al.*, Phys. Rev. **D85**, 081101 (2012), 1112.4940.
- [48] F. Beutler, C. Blake, M. Colless, D. H. Jones, L. Staveley-Smith, *et al.*, Mon.Not.Roy.Astron.Soc. **416**, 3017 (2011), 1106.3366.
- [49] A. J. Ross, L. Samushia, C. Howlett, W. J. Percival, A. Burden, *et al.* (2014), 1409.3242.
- [50] L. Anderson *et al.* (BOSS Collaboration) (2013), 1312.4877.
- [51] P. Ade *et al.* (Planck Collaboration) (2013), 1303.5076.
- [52] A. Font-Ribera *et al.* (BOSS Collaboration), JCAP (2013), 1311.1767.
- [53] A. Liu, J. R. Pritchard, R. Allison, A. R. Parsons, U. Seljak, and B. D. Sherwin (2015), 1509.08463.
- [54] R. Allison, P. Caucal, E. Calabrese, J. Dunkley, and T. Louis, ArXiv e-prints (2015), 1509.07471.
- [55] M. Betoule, R. Kessler, J. Guy, J. Mosher, D. Hardin, R. Biswas, P. Astier, P. El-Hage, M. Konig, S. Kuhlmann, J. Marriner, R. Pain, *et al.*, A&A **568**, A22 (2014), 1401.4064.
- [56] A. G. Riess, L. Macri, S. Casertano, H. Lampeitl, H. C. Ferguson, A. V. Filippenko, S. W. Jha, W. Li, and R. Chornock, ApJ **730**, 119 (2011), 1103.2976.
- [57] A. J. Cuesta, L. Verde, A. Riess, and R. Jimenez, MNRAS **448**, 3463 (2015), 1411.1094.
- [58] C. Heymans *et al.*, Mon. Not. Roy. Astron. Soc. **427**, 146 (2012), 1210.0032.
- [59] T. Erben *et al.*, Mon. Not. Roy. Astron. Soc. **433**, 2545 (2013), 1210.8156.
- [60] B. Leistedt, H. V. Peiris, and L. Verde, Physical Review Letters **113**(4), 041301 (2014), 1404.5950.
- [61] F. Beutler *et al.* (BOSS), Mon. Not. Roy. Astron. Soc. **444**, 3501 (2014), 1403.4599.
- [62] L. Samushia *et al.*, Mon. Not. Roy. Astron. Soc. **439**(4), 3504 (2014), 1312.4899.
- [63] N. Haba and R. Takahashi, Acta Phys. Polon. **B45**(1), 61 (2014), 1305.0147.